A Method of SSVEP Signal Identification Based on Improved eCAA

LI Jiaxin, DAI Fengzhi*, YIN Di, LU Peng, WEN Haokang

(*College of Electronic Information and Automation*, *Tianjin University of Science and Technology*, *Tianjin 300222*, *China*)

Abstract: Brain-computer interfaces (BCI) based on steady-state visual evoked potentials (SSVEP) have attracted great interest because of their higher signal-to-noise ratio, less training, and faster information transfer. However, the existing signal recognition methods for SSVEP do not fully pay attention to the important role of signal phase characteristics in the recognition process. Therefore, an improved method based on extended Canonical Correlation Analysis (eCCA) is proposed. The phase parameters are added from the stimulus paradigm encoded by joint frequency phase modulation to the reference signal constructed from the training data of the subjects to achieve phase constraints on eCCA, thereby improving the recognition performance of the eCCA method for SSVEP signals, and transmit the collected signals to the robotic arm system to achieve control of the robotic arm. In order to verify the effectiveness and advantages of the proposed method, this paper evaluated the method using SSVEP signals from 35 subjects. The research shows that the proposed algorithm improves the average recognition rate of SSVEP signals to 82.76%, and the information transmission rate to 116.18 bits/min, which is superior to TRCA and traditional eCAA-based methods in terms of information transmission speed and accuracy, and has better stability.

Keywords: Brain-computer Interface, Electroencephalographic Signal, Extended Canonical Correlation Analysis (eCCA), Manipulator, Steady State Visual Evoked Potential

1 Introduction

The principle of Brain Computer Interface (BCI) is to create a communication and control channel between the brain and the external environment, enabling direct signal interaction between the brain and external devices[1−3]. Existing computer-based BCI systems acquire, analyze, and convert EEG signals into output signals for control of external devices. The BCI system consists of three main components: (1) acquisition signal, i.e., the acquisition of EEG signals from the user; (2) signal processing, i.e., the extraction and classification of EEG signal features according to the user's intention; and (3) output signal, i.e., the system sends control signals to make external devices perform a series of actions according to the user’s intention[4].

Many studies have shown that Steady-State Visual Evoked Potential (SSVEP) is a stable electroencephalographic oscillation evoked by periodic stimuli of high frequency, i.e., a significant SSVEP signal can be detected in the occipital region of the cerebral cortex when subjects are subjected to visual stimuli that flicker periodically at a certain frequency. The EEG signal of SSVEP has a frequency component which like the stimulus frequency and its higher harmonic components[5–6]. Therefore, the spectral peaks at the stimulus frequencies or harmonics can be seen in the EEG signal after power spectroscopy, and the frequency components corresponding to the spectral peaks can be analyzed to know the components of the stimulus source that the subject is looking at, and thus the intention of the activity that the subject wants to express.

The interference of some spontaneous brain activities when detecting EEG signals is inevitable. Effective feature extraction of EEG signals is not only the key to accurately identify the frequency of SSVEP in a short time, but also the key to further develop high-performance brain computer interfaces based on SSVEP. Typical correlation analysis (CCA) is a commonly used method for signal identification[7–8]. Therefore, Lin et al[9] firstly applied CCA to signal feature extraction of SSVEP-BCI system, analyzed the relationship between multichannel SSVEP EEG signals and reference signals, and calculated the maximum correlation coefficient between them. Compared with the traditional power spectral density analysis method, the CCA-based method can significantly improve the frequency identification performance. Chen et al[10] introduced extended typical correlation analysis (eCAA) to combine CCA coefficients with Pearson correlation coefficients of test and training data. Mohammand et al[11] proposed a new CCA-based approach which improves the performance of BCI systems by using subject-specific and subject-independent training methods. In addition, task-related component analysis (TRCA) has been one of the most popular methods for SSVEP identification in recent years. Therefore, Nakanishi M et al[12] introduced the TRCA method into SSVEP to improve the signal-to-noise ratio and suppress spontaneous EEG activity by maximizing the recurrence between multiple tasks.

The extended CCA and TRCA methods have significant advantages in classification accuracy, short time windows, and ITR[13]. Therefore, in the second section of this article, a constraint recognition algorithm based on the relationship between eCCA and the reference signal is proposed. This algorithm adds the stimulus paradigm design parameters of SSVEP to the reference signal, and in the third section, the collected EEG signal is transmitted to the robot arm system to control the robot arm to execute specified commands[14]. In order to verify the effectiveness of the proposed method, a comparative study was conducted in the fourth section between the TRCA algorithm and the traditional eCCA algorithm based on publicly available EEG data from Tsinghua University.

2 Method

2.1 The eCCA

The principle of the CCA algorithm is to first analyze the relationship between multi-channel SSVEP EEG signals and reference signals of each stimulus frequency, and then infer the maximum correlation coefficient between them, in order to obtain the corresponding output control instructions for the stimulus target and SSVEP signals. It is an unsupervised method that does not use any pre obtained data to train the system. Numerous studies[15] have found that incorporating subject training data into SSVEP signal recognition methods can more effectively capture the temporal characteristics of SSVEP responses and improve the performance of CCA based methods. Three types of multi-channel information can be obtained through the training data of the subjects [16]:

(1) Test data X ;

(2) The template signal X_k obtained from the average of the training data of the kTH subject;

(3) Sine and cosine reference signal Y_k .

By calculating the CCA between each pair of the three types of multi-channel information mentioned above, 6 spatial filters can be generated, resulting in 10 typical variables[17]. Then, a total of 45 correlation features between two typical variables are calculated, and 36 of the effective correlation features can be used for SSVEP signal recognition.

Chen et al[12] proposed an eCCA method by combining the Pearson correlation coefficients of CCA and subject training data: by selecting 5 correlation features $r_k(i), i=1, 2, 3, 4, 5$, between test data x and template signal $\hat{X}_k$, the feature set with the best signal recognition performance is constructed:

$$\boldsymbol{r}_k=\begin{bmatrix}\boldsymbol{r}_k(1)\\ \boldsymbol{r}_k(2)\\ \boldsymbol{r}_k(3)\\ \boldsymbol{r}_k(4)\\ \boldsymbol{r}_k(5)\end{bmatrix}=\begin{bmatrix}\rho(\boldsymbol{X}^T\boldsymbol{W}_X(\boldsymbol{X}\boldsymbol{Y}_k),\ \boldsymbol{Y}_k^T\boldsymbol{W}_{\boldsymbol{Y}_k}(\boldsymbol{X}\boldsymbol{Y}_k))\\ \rho(\boldsymbol{X}^T\boldsymbol{W}_X(\boldsymbol{X}\hat{\boldsymbol{X}}_k),\ \hat{\boldsymbol{X}}_k^T\boldsymbol{W}_X(\boldsymbol{X}\hat{\boldsymbol{X}}_k))\\ \rho(\boldsymbol{X}^T\boldsymbol{W}_X(\boldsymbol{X}\boldsymbol{Y}_k),\ \hat{\boldsymbol{X}}_k^T\boldsymbol{W}_X(\boldsymbol{X}\boldsymbol{Y}_k))\\ \rho(\boldsymbol{X}^T\boldsymbol{W}_{\hat{\boldsymbol{X}}_k}(\hat{\boldsymbol{X}}_k\boldsymbol{Y}_k),\ \hat{\boldsymbol{X}}_k^T\boldsymbol{W}_{\hat{\boldsymbol{X}}_k}(\hat{\boldsymbol{X}}_k\boldsymbol{Y}_k))\\ \rho(\hat{\boldsymbol{X}}_k^T\boldsymbol{W}_X(\boldsymbol{X}\hat{\boldsymbol{X}}_k),\ \hat{\boldsymbol{X}}_k^T\boldsymbol{W}_{\hat{\boldsymbol{X}}_k}(\boldsymbol{X}\hat{\boldsymbol{X}}_k))\end{bmatrix} \tag{1}$$

Where $\rho(a, b)$ represents the relevant features of a and b, and $\boldsymbol{W}_A(AB)$ represents the spatial filter between two multi-channel information A and B calculated by CCA. Use the weighted sum of squares of these five related features as the final feature representation for signal recognition[18–19]:

$$\rho_k=\sum_{i=1}^{5}sign(r_k(i))*(r_k(i))^2 \tag{2}$$

Among them, *sign*() is used to preserve the discriminative information of the negative correlation coefficient between the test set X and the training data template signal $\hat{X}_k$. By confirming the stimulus corresponding to the maximum correlation coefficient, target recognition and classification can be achieved.

Mohammand et al[11] selected 6 correlation features $r_k(i),\ i=1,\ 2,\ 3,\ 4,\ 5,\ 6$ out of 36 effective correlation features to construct the feature set with the best signal recognition performance:

$$\boldsymbol{r}_k=\begin{bmatrix}\boldsymbol{r}_k(1)\\ \boldsymbol{r}_k(2)\\ \boldsymbol{r}_k(3)\\ \boldsymbol{r}_k(4)\\ \boldsymbol{r}_k(5)\\ \boldsymbol{r}_k(6)\end{bmatrix}=\begin{bmatrix}\rho(\boldsymbol{X}^T\boldsymbol{W}_X(\boldsymbol{X}\boldsymbol{Y}_k),\ \boldsymbol{Y}_k^T\boldsymbol{W}_{\boldsymbol{Y}_k}(\boldsymbol{X}\boldsymbol{Y}_k))\\ \rho(\boldsymbol{X}^T\boldsymbol{W}_X(\boldsymbol{X}\hat{\boldsymbol{X}}_k),\ \hat{\boldsymbol{X}}_k^T\boldsymbol{W}_{\hat{\boldsymbol{X}}_k}(\boldsymbol{X}\hat{\boldsymbol{X}}_k))\\ \rho(\boldsymbol{X}^T\boldsymbol{W}_X(\boldsymbol{X}\hat{\boldsymbol{X}}_k),\ \hat{\boldsymbol{X}}_k^T\boldsymbol{W}_X(\boldsymbol{X}\hat{\boldsymbol{X}}_k)\\ \rho(\boldsymbol{X}^T\boldsymbol{W}_X(\boldsymbol{X}\boldsymbol{Y}_k),\ \hat{\boldsymbol{X}}_k^T\boldsymbol{W}_X(\boldsymbol{X}\boldsymbol{Y}_k)\\ \rho(\boldsymbol{X}^T\boldsymbol{W}_{\hat{\boldsymbol{X}}_k}(\hat{\boldsymbol{X}}_k\boldsymbol{Y}_k),\ \hat{\boldsymbol{X}}_k^T\boldsymbol{W}_{\hat{\boldsymbol{X}}_k}(\hat{\boldsymbol{X}}_k\boldsymbol{Y}_k)\\ \rho(\boldsymbol{X}^T\boldsymbol{W}_{\hat{\boldsymbol{X}}_k}(\hat{\boldsymbol{X}}_k\boldsymbol{Y}_k),\ \boldsymbol{Y}_k^T\boldsymbol{W}_{\boldsymbol{Y}_k}(\hat{\boldsymbol{X}}_k\boldsymbol{Y}_k)\end{bmatrix} \tag{3}$$

Use the sum of these six related features as the final feature representation for signal recognition:

$$\rho_k=\sum_{i=1}^{6}\boldsymbol{r}_k(i) \tag{4}$$

2.2 The eCCA-Y

Among the two feature combinations proposed by Mohammand et al[11] and Chen et al[11] six combinations of correlation coefficients can be obtained. Considering the final accurate recognition rate and ITR, we chose four correlation coefficients for the combination of correlation coefficients in this experiment, and the combination equation is as follows.

$$\boldsymbol{r}_k=\begin{bmatrix}\boldsymbol{r}_k(1)\\ \boldsymbol{r}_k(2)\\ \boldsymbol{r}_k(3)\\ \boldsymbol{r}_k(4)\end{bmatrix}=\begin{bmatrix}\rho(\boldsymbol{X}^T\boldsymbol{W}_X(\boldsymbol{X}\boldsymbol{Y}_k),\ \boldsymbol{Y}_k^T\boldsymbol{W}_{\boldsymbol{Y}_k}(\boldsymbol{X}\boldsymbol{Y}_k))\\ \rho(\boldsymbol{X}^T\boldsymbol{W}_X(\boldsymbol{X}\hat{\boldsymbol{X}}_k),\ \hat{\boldsymbol{X}}_k^T\boldsymbol{W}_X(\boldsymbol{X}\hat{\boldsymbol{X}}_k))\\ \rho(\boldsymbol{X}^T\boldsymbol{W}_X(\boldsymbol{X}\boldsymbol{Y}_k),\ \hat{\boldsymbol{X}}_k^T\boldsymbol{W}_X(\boldsymbol{X}\boldsymbol{Y}_k))\\ \rho(\boldsymbol{X}^T\boldsymbol{W}_{\hat{\boldsymbol{X}}_k}(\hat{\boldsymbol{X}}_k\boldsymbol{Y}_k),\ \hat{\boldsymbol{X}}_k^T\boldsymbol{W}_{\hat{\boldsymbol{X}}_k}(\hat{\boldsymbol{X}}_k\boldsymbol{Y}_k))\end{bmatrix} \tag{5}$$

After simplifying and transforming the formula, the coefficients of the k-th stimulus frequency can be obtained, calculated as follows, and then classified using the maximum correlation coefficient.

$$\rho_k=\sum_{i=1}^{4}sign(\boldsymbol{r}_k(i))*(\boldsymbol{r}_k(i))^2 \tag{6}$$

Phase information is only reflected in the subject's EEG signal training data, and there is no phase information present in the constructed fitting signal. Therefore, the eCCA-Y algorithm is proposed based on eCCA, and the phase in the SSVEP stimulus paradigm is added to the reference signal[20–21], and the constrained reference signal is represented as follows:

$$\boldsymbol{Y}_{f_k,\theta_k}=\begin{bmatrix}\sin(2\pi f_k t+\theta_k)\\ \cos(2\pi f_k t+\theta_k)\\ \vdots\\ \sin(2\pi N_h f_k t+N_h\theta_k)\\ \cos(2\pi N_h f_k t+N_h\theta_k)\end{bmatrix}^T,\ t=\frac{1}{F_s},\ \frac{2}{F_s},\ \cdots,\ \frac{N_t}{F_s} \tag{7}$$

where Y_{f_k,θ_k} is the reference signal containing the phase information θ_k of the kth frequency stimulus (if $\theta_k=0$, it is the reference signal of CCA). In a practical experiment, depending on the experimental intent, the researcher can design the stimulus paradigm to determine the magnitude of θ_k as follows.

$$\theta_k=\theta_0+\Delta\theta\times\left[(k_y-1)\times 5+(k_x-1)\right] \tag{8}$$

where k_x and k_y denote the row and column indices of the visual stimulus matrix, respectively, θ_0 denotes the initial phase, and $\Delta\theta$ denotes the phase interval.

For the fundamental component, the signal fitted by the linear combination of the sine and cosine reference signal has the same frequency but usually has a non-zero phase. EEG signal data are estimated by maximizing the correlation between the test data and the reference signal, i.e., the data are too short and overfitting is likely to occur. A fixed SSVEP response phase exists for each stimulus frequency, and the proposed method can be used to constrain the eCCA to improve the classification performance in frequency identification.

3 Application Research of Manipulator Based on SSVEP-BCI Control

3.1 Experiment of Robotic Arm Based on SSVEP-BCI

The BCI EEG acquisition system communicates with the robot system through UDP protocol. The EEG acquisition equipment is responsible for generating control instructions that the robotic arm can recognize by converting the recorded EEG signals through analog-to-digital conversion and online processing (obtain relevant features and convert them in real-time through algorithms).

The EEG acquisition system based on SSVEP-BCI is programmed using the PSYCHTOOLBOX (PTB) toolbox[22] in MATLAB to form specific stimulus paradigms for some inherent actions of the robotic arm. PTB can create stimuli, present stimuli, and record data as functions. Fig.1 (a) is the final motivational paradigm of the model, which displays the images seen by the subjects in order: forward, towards the left, towards the right, and upward; backward, counterclockwise rotation, clockwise side rotation, downward; Grab, release, and stop, Fig.1 (b) shows their different frequencies and phases under the stimulus mode.

When collecting EEG data, parallel port interfaces are usually used, and Pin2-9 can write data (used for sending stimulus codes in EEG experiments) with 8 data bits,. In EEG experiments, different frequency recognition will be marked, and PortTalk's Inpout will be used to create registers to access possible drivers or call parallel port pins. MATLAB's data collection toolbox can automatically read the port address from the Windows memory protection area containing BIOS data.

After collecting EEG signals, the BCI system undergoes real-time processing and connects to control devices through UDP protocol.

3.2 Experiment of Robotic Arm Based on SSVEP-BCI

The SSVEP data used was from 35 subjects, 17 female and 18 male, with a mean age of 22 years. 8 individuals have previous experience with SSVEP experiments and the remaining 27 individuals have no experience. All subjects are in good health and had normal (or corrected normal) vision. The experiment is shown in Fig.2.

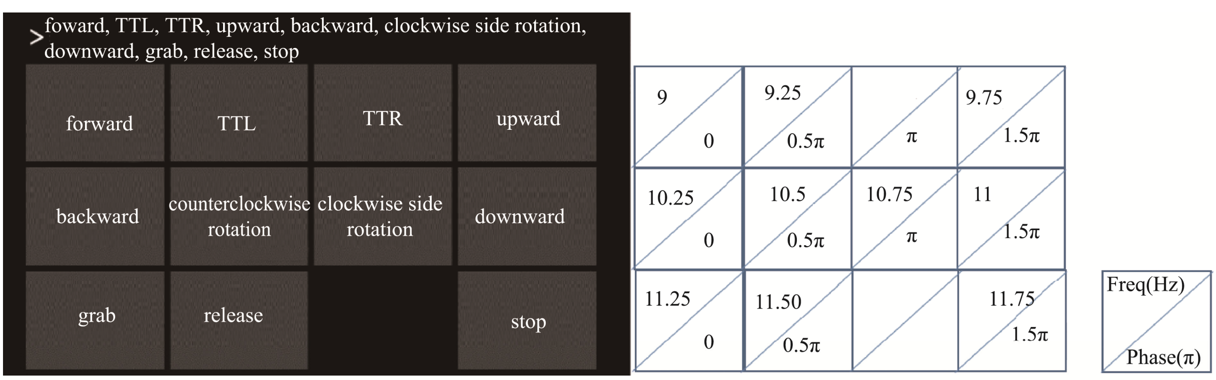

(a) Mechanical Arm Motion Diagram (b) Corresponding Phase

Fig.1 Mechanical Arm Excitation Model

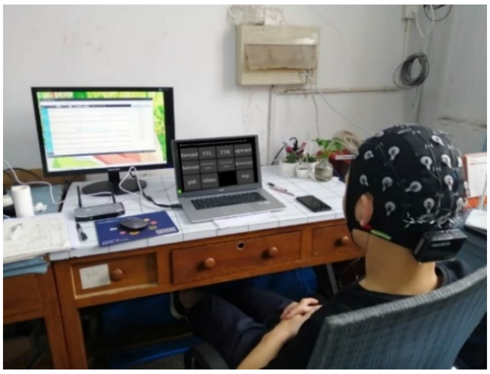

Fig.2 Subjects Conducting SSVEP Experiments

The EEG acquisition device used in this trial is a 64-channel EEG cap from Neuroscan's Synamps2 system with a sampling rate of 1000 Hz. the electrodes of the EEG cap are set up according to the international 10-20 system. Nine channels of Pz, PO5, PO3, POz, PO4, PO6, O1, Oz, and O2 are selected. As shown in Fig.3, the electrode positions of the parietal lobe were marked with the letter P, and the electrode positions of the occipital lobe were marked with the letter O, because the scalp topography of SSVEP showed high activity in the parietal and visual regions[23].

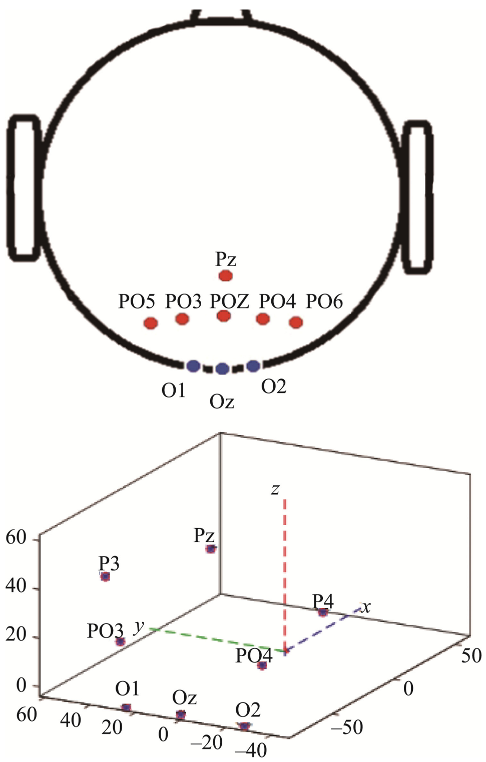

Fig.3 Electrode Channel Diagram

Five subjects (4 males and 1 female) were selected from a large sample, and a total of five groups (blocks) were conducted for each subject, with 11 goals in each group. The stimulation frequencies corresponding to the positions of the 11 targets on the screen were 9Hz, 9.25Hz, 9.5Hz, 9.75Hz, 10.25Hz, and 10.5Hz, 10.75Hz, 11Hz, 11.25Hz, 11.5Hz, and 11.75Hz.

Traverse 11 targets in sequence, with each target stimulus lasting for 5 seconds (with stimulus prompt for 0.5 seconds and stimulus flicker for 4.5 seconds). Each time the target flickers, the subjects try to avoid blinking. Therefore, after each experiment, in order to avoid visual fatigue for the subjects, they rest for 2-3 minutes. The experimental arrangement of the test data is shown in Table 1.

Table 1 Experimental Arrangement of Test Data

0.5s	4.5s	0.5s	4.5s	0.5s	…	0.5s	4.5s
9Hz		9.25Hz		…		11.75Hz	
Trial1		Trial2		…		Trial11	
55s							

Through data preprocessing, 8 signal channels (Pz, PO3, POz, PO4, PO6, O1, Oz, and O2) were extracted, and filtered to obtain three-dimensional EEG data (channels * points * experiments). In order to enhance the effectiveness of the data, the experimental group (block) was combined with three-dimensional EEG data to obtain four-dimensional data (channel * point * test * block), which was downsampled from 1000Hz to 250Hz. Each experiment consists of 3000 sampling points, which form EEG data of 8 * 750 * 11 * 5.

EEG data recorded through non-invasive devices can be considered as the sum of real EEG signals and artifacts, which are independent of each other. In order to remove artifacts from EEG data, the calculated independent components are first divided into artificial or neural related components[24]. If independent components related to artifacts are detected and marked, they can be eliminated and the remaining data remixed. Fig.4 is an independent component analysis (ICA) diagram after elimination.

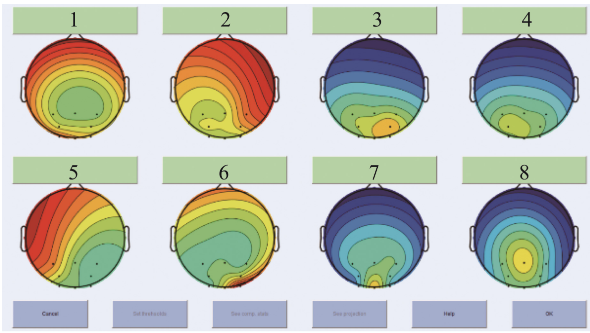

Fig.4 ICA Components after Elimination

Continuous EEG data will be available for 6s per trial. 1000Hz downsampled to 250Hz. Therefore, each trial will contain 1500 sampling points, and given the 140ms latency of the visual pathway system, all time periods will be extracted in intervals [0.14s, 0.14+ds], this is because the 140ms after SSVEP stimulation is a transient component, and only subsequently reaches a steady-state component. However, the phase of the steady-state component is shifted as the event changes. Therefore, a bandpass filter (Butterworth filter) of 6Hz-90Hz was used for filtering[25].

3.3 Simulation of Manipulator Based on SSVEP-BCI

The EEG acquisition system and robot system are two important components of SSVEP-BCI [26–28]. Transform the subject's EEG signals for feature extraction and recognition into controlling the motion of the robotic arm end effector, enabling the robotic arm to complete grasping and moving movements.

Before using SSVEP-BCI to control the manipulator, the six degrees of freedom manipulator was simulated and developed on the combined platform of VC9 and OpenGL. OpenGL software control interface is shown in Fig.5.

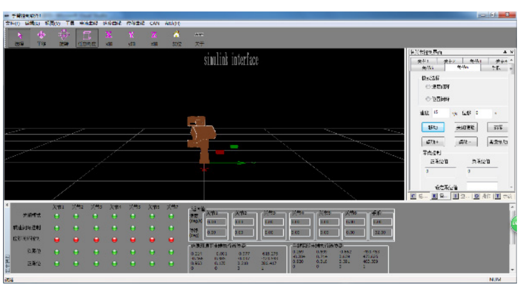

Fig.5 OpenGL Software Control Interface

The robotic arm is shown in Fig.6. After transmitting EEG signals to the upper computer, the joints of the robotic arm begin to perform calibration actions. By controlling the circuit, various joint angles of the robotic arm are controlled and the relative position of each servo mechanism is detected. Define the angle and action execution time of each servo through the upper computer to execute the corresponding actions of the robotic arm.

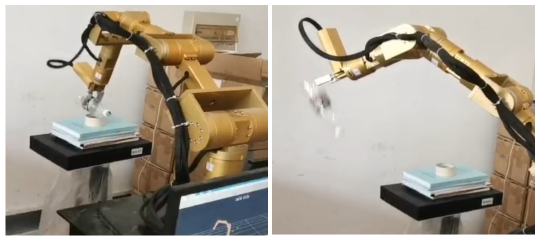

Fig.6 Physical Image of the Robotic Arm

4 Result

4.1 Performance Comparison of Three Related Algorithms

Identify the average accuracy and average ITR of 35 subjects, and compare the effectiveness of the three algorithms under time window lengths of 0.5s, 1s, 1.5s, 2s, and 2.5s, as shown in Fig.7.

In (a) of Fig.7, among the three algorithms (TRCA, eCCA, and eCCA-Y), the eCCA and eCCA-Y algorithms have higher average recognition rates than TRCA for 35 subjects in different time window lengths. The proposed improved constrained eCCA algorithm (eCCA-Y) has higher recognition rates than TRCA and eCCA in most time windows. It can be seen in (b) that the average ITR of the eCCA-Y algorithm is significantly higher than that of TRCA and shows a small improvement over the eCAA algorithm for most of the time window lengths. When TW < 1.5s, the proposed method outperforms both TRCA and eCCA methods; however, both show an inflection point at the time window length of 1.5s, and both show an increasing trend until 1.5s, and decrease at the time window length of 2s. Therefore, the time window length of 1.5s with 375 sampling points is considered for this dataset.

For eCCA algorithm, the number of harmonics is a factor in determining its performance. For TRCA, the phase information is included in the time domain average of its trials, so there is no harmonic count selection. Therefore, this paper only compares the harmonic components of both eCCA and eCCA-Y algorithms, as shown in Fig.8.

As it can be seen in (a) of Fig.8, the average recognition rate of 35 subjects tends to a stable value at harmonic number 2; (b) shows that it rises quickly to more than 110 bits/min at harmonic number 2, drops abruptly at harmonic number 3, and subsequently tends to a stable state. Therefore, when comparing the algorithm performance, the harmonic number 2 is chosen for SSVEP target identification.

The validation method used in this paper is Leave-One-Out Cross Validation (LOOCV)[29], which aims to estimate the recognition rate and ITR for each experiment. The number of harmonics is taken as 2, the number of channels is 9, and the time window length is 1.5s in the analysis, so the EEG data of 1.5s is intercepted in the sampling point 1500. Table 2 compares the recognition accuracy and ITR of TRCA, eCCA, and the proposed algorithm eCCA-Y method.

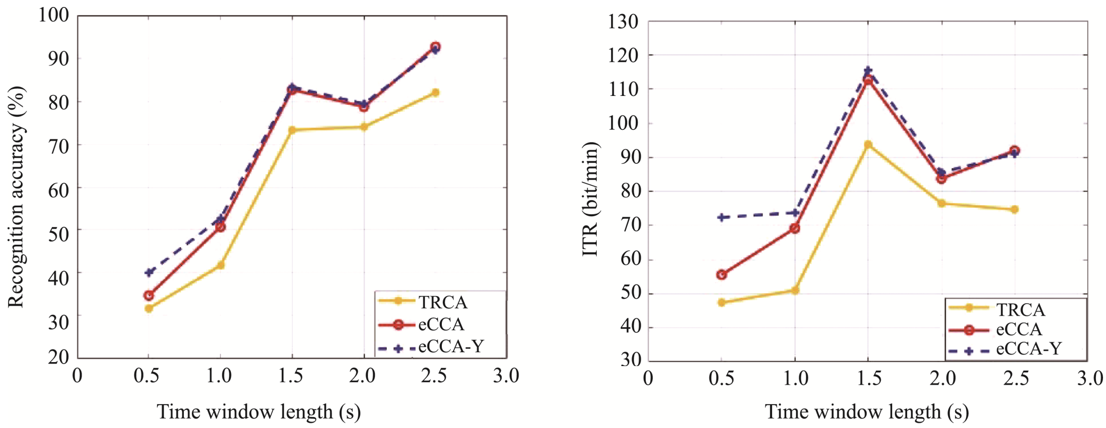

(a) Average Recognition Rate for Different Window Lengths (b) Average ITR for Different Window Lengths

Fig.7 Performance of 3 Algorithms with Different Window Lengths

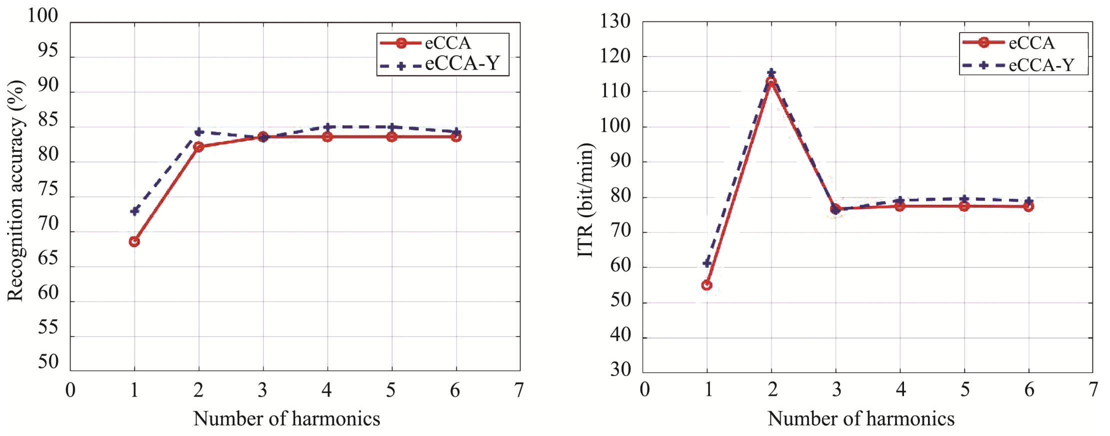

(a) Average Recognition Rate of Different Harmonic Numbers (b) Average ITR of Different Harmonic Numbers

Fig.8 Algorithm Performance of Different Harmonic Orders

Table 2 Comparison of Classification Accuracy and ITR of Each Algorithm

Subject	Correct Rate (%)			ITR (bits/min)		
	TRCA	eCCA	eCCA-Y	TRCA	eCCA	eCCA-Y
S1	66.67	73.33	**75.42**	79.47	92.69	**97.01**
S2	48.33	50	**72.93**	48.28	50.89	**91.56**
S3	98.33	**98.75**	**98.75**	154.25	**155.4**	**155.4**
S4	87.5	**88.33**	87.92	123.74	**125.94**	124.77
S5	73.33	92.08	**93.33**	92.94	135.5	**138.77**
S6	73.75	82.5	**83.75**	93.8	112.88	**115.45**
S7	70.83	**79.17**	78.33	87.91	**105.25**	103.3
S8	85.83	86.67	**89.17**	119.92	122	**127.99**
S9	68.33	75	**76.25**	83.48	96.3	**99.12**
S10	56.25	71.67	**72.5**	60.74	89.51	**91.08**
S11	65.42	**82.5**	81.67	77.15	**112.3**	110.49
S12	65.42	86.67	**88.33**	77.31	122.15	**126.63**
S13	73.33	**85.83**	85	93.37	**119.94**	117.72
S14	**98.75**	98.33	**98.75**	**155.15**	153.64	**155.15**
S15	67.08	**83.75**	82.92	80.15	**115.74**	113.79
S16	48.75	50	**52.92**	48.99	51.07	**55.92**
S17	75.83	**81.67**	81.25	97.14	**110.67**	109.46
S18	88.33	**89.58**	**89.58**	127.97	129.41	**129.73**
S19	36.25	53.33	**53.75**	29.39	56.04	**56.57**
S20	95.42	**97.08**	96.67	145.73	**149.89**	149.1
S21	54.58	67.92	**93.75**	58.22	82.05	**140.49**
S22	96.25	97.08	**97.5**	147.24	149.89	**151.14**
S23	63.75	70	**73.75**	75.29	86	**93.58**
S24	85.83	87.92	**89.17**	120.2	125.76	**128.73**
S25	95.83	**97.92**	97.08	145.74	**152.99**	149.89
S26	89.17	**93.75**	92.5	128.46	**139.85**	136.58
S27	75	80.42	**82.08**	94.91	108.75	**111.98**
S28	**97.08**	94.17	94.17	**149.64**	141.8	141.22
S29	41.25	47.5	**47.92**	37.65	46.87	**47.3**
S30	57.08	67.92	**70**	62.61	82.46	**86.98**
S31	**98.33**	**98.33**	**98.33**	**154.25**	153.64	153.64
S32	**95**	93.75	93.75	**143.34**	140.67	140.77
S33	27.5	40.83	**41.25**	18.59	37.01	**37.89**
S34	92.5	**97.5**	90	136.74	**151.4**	130.18
S35	**96.67**	**96.67**	96.25	148.14	**148.49**	146.99
Mean ±Standard Deviation	74.56±19.4	81.08±16.46	82.76±14.96	99.94±40.16	113±34.65	116.18±31.6

As can be seen from Table 2, the accuracy of each subject under the TRCA algorithm varied, with the highest accuracy being 98.74% and the smallest being 27.5%. The attention of each subject and the difference in EEG signal feedback were factors that affected the recognition rate. The average accuracy of all subjects was 74.6 ± 19.4% and the average ITR was 99.94 ± 40.15 bit/min. Compared with the TRCA feature method, eCCA showed a significant improvement in recognition rate and ITR, with an average accuracy of 81.08 ± 16.46% and an average ITR of 113 ± 34.65 bit/min for all subjects. The run data of eCCA-Y algorithm showed an average accuracy of 82.76 ± 14.96% and an average ITR of 116.18 ± 31.6 bits/min for all subjects, which was improved for most subjects compared to the first two algorithms.

The average accuracy and average ITR of the 35 subjects were plotted as line graphs to compare the performance of these three algorithms, as shown in Fig.9.

Through Fig.9 we can find that the recognition rate and ITR of eCCA-Y are significantly higher than those of TRCA, with a recognition rate increase of about 13%. eCCA-Y has a slightly higher recognition rate and ITR than eCCA, with an average recognition rate of 2.1% higher than that of eCCA, and its ITR also increases by 2.8%.

4.2 The Recognition Accuracy of EEG Signals in Robotic Arm Systems

The experiment analyzed the data of 5 subjects and compared the harmonic quantity and time window data. Finally, a sample point with a harmonic quantity of 2 and a data length of 750 was selected to compare the classification performance of eCCA and eCCA-Y algorithms, as shown in Fig.10.

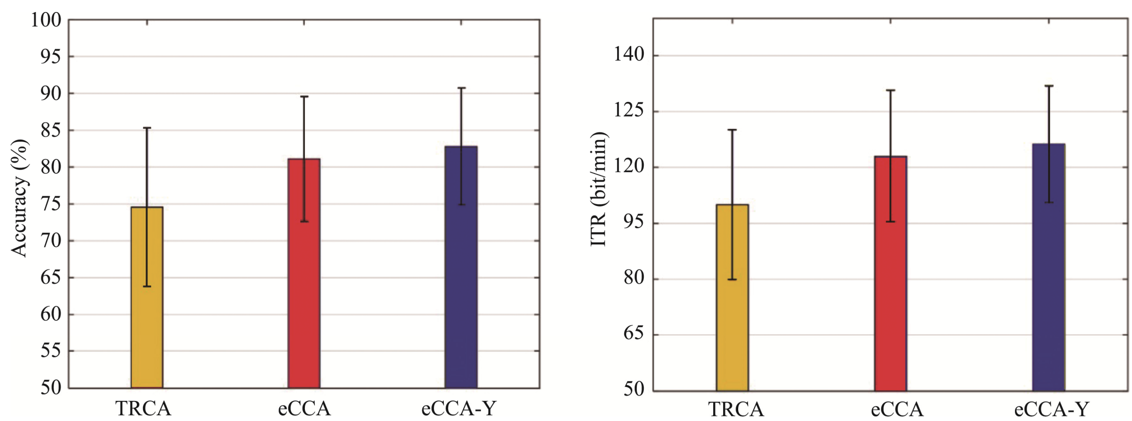

Fig.9 Performance Evaluation of 3 Algorithms

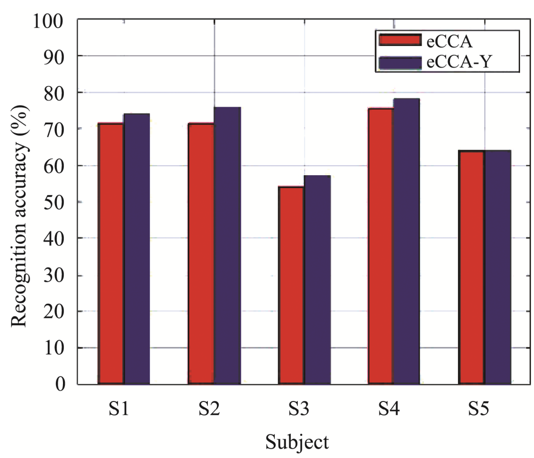

(a) The Recognition Accuracy of the Subjects

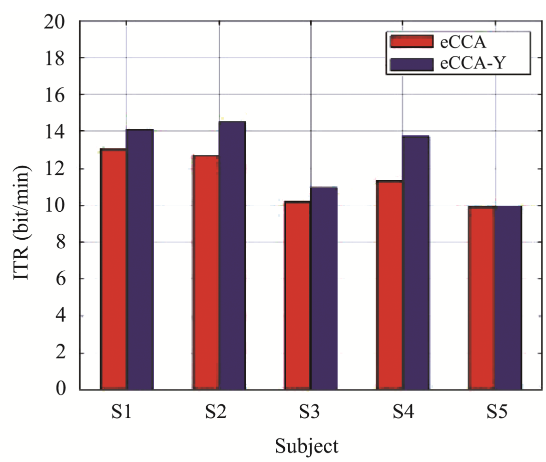

(b) The ITR of the Subjects

Fig.10 Application Performance Evaluation of Different Algorithms

From Fig.10 (a), it can be seen that the eCCA-Y algorithm has a higher recognition rate than the eCCA algorithm. S5 indicates that the accuracy of both is the same, while S3 has a lower recognition rate compared to the other four subjects. As shown in Fig.10 (b), both eCCA-Y and eCCA have improved their ITR. The maximum difference in ITR was observed among S4 subjects.

5 Conclusion

In order to improve the frequency recognition performance of SSVEP, this paper proposes an eCCA based constrained eCCA method (eCCA-Y), which adds SSVEP stimulus paradigm design parameters to the reference signal and inputs the signal into the robotic arm system to achieve control of the robotic arm. The results indicate that the eCCA-Y algorithm in the SSVEP frequency recognition method can effectively improve the frequency recognition accuracy of SSVEP in the case of short Time Window, and can be applied to robotic arm systems.

References

[1] Vidal, J. J.. (1973). Towards direct brain-computer communication. Annu Rev Biophys Bioeng, 2, 157-180.

[2] Jonathan R Wolpaw, Niels Birbaumer, Dennis J McFarland... & Theresa M Vaughan. (2002).Brain–computer interfaces for communication and control. Clinical Neurophysiology (6). doi:10.1016/S1388-2457(02)00057-3.

[3] Middendorf, M., Mcmillan, G., Calhoun, G., & Jones, K. S.. (2000). Brain-computer interfaces based on the steady-state visual-evoked response. IEEE transactions on rehabilitation engineering (2), 8.

[4] Musk Elon. (2019).An Integrated Brain-Machine Interface Platform With Thousands of Channels.. Journal of medical Internet research (10). doi:10.2196/16194.

[5] Müller-Putz Gernot R, Scherer Reinhold, Brauneis Christian & Pfurtscheller Gert. (2005).Steady-state visual evoked potential (SSVEP)-based communication: impact of harmonic frequency components.. Journal of neural engineering (4).

[6] Cheng, M., Gao, X., Gao, S., & Xu, D.. (2002). Design and implementation of a brain-computer interface with high transfer rates. IEEE Transactions on Biomedical Engineering (10), 49.

[7] Emmanuel K. Kalunga, Sylvain Chevallier, Quentin Barthélemy... & Yskandar Hamam. (2016).Online SSVEP-based BCI using Riemannian geometry. Neurocomputing. doi: 10.1016/j.neucom.2016.01.007.

[8] Yu Zhang, Guoxu Zhou, Jing Jin... & Andrzej Cichocki. (2017).Sparse Bayesian multiway canonical correlation analysis for EEG pattern recognition. Neurocomputing. doi: 10.1016/j.neucom.2016.11.008.

[9] Lin Zhonglin, Zhang Changshui, Wu Wei & Gao Xiaorong. (2006).Frequency recognition based on canonical correlation analysis for SSVEP-based BCIs.. IEEE transactions on bio-medical engineering (12 Pt 2). doi:10.1109/TBME.2006.886577.

[10] Chen, X., Wang, Y., Nakanishi, M., Gao, X., Jung, T. P., & Gao, S.. (2015). High-speed spelling with a noninvasive brain–computer interface. National Academy of Sciences (44).

[11] Mehdizavareh Mohammad Hadi, Hemati Sobhan & Soltanian-Zadeh Hamid. (2020). Enhancing performance of subject-specific models via subject-independent information for SSVEP-based BCIs.. PloS one (1). doi: 10.1371/journal.pone.0226048.

[12] Nakanishi, M., Wang, Y., Chen, X., Wang, Y. T., Gao, X., & Jung, T. P.. (2017). Enhancing detection of ssveps for a high-speed brain speller using task-related component analysis. IEEE transactions on bio-medical engineering, 1-1.

[13] Nakanishi, M., Wang, Y., Wang, Y. T., & Jung, T. P.. (2015). A comparison study of canonical correlation analysis based methods for detecting steady-state visual evoked potentials. PLOS ONE.

[14] Douibi, K., Bars, S. L., Lemontey, A., Nag, L., Balp, R., & Breda, G.. (2021). Toward EEG-based bci applications for industry 4.0: challenges and possible applications. Frontiers in Human Neuroscience, 15, 456-.

[15] Hirokazu Tanaka, Takusige Katura & Hiroki Sato. (2013).Task-related component analysis for functional neuroimaging and application to near-infrared spectroscopy data. NeuroImage (1). doi: 10.1016/j.neuroimage.2012.08.044.

[16] Robbin A. Miranda, William D. Casebeer, Amy M. Hein... & Geoffrey S.F. Ling. (2015). DARPA-funded efforts in the development of novel brain–computer interface technologies. Journal of Neuroscience Methods. doi: 10.1016/j.jneumeth.2014.07.019.

[17] Ou Bai, Peter Lin, Sherry Vorbach, Mary Kay Floeter, Noriaki Hattori & Mark Hallett. (2008).A high performance sensorimotor beta rhythm-based brain–computer interface associated with human natural motor beha-

vior. Journal of Neural Engineering (1). doi:10.1088/1741-2560/5/1/003.

[18] Zerafa, R., Camilleri, T., Falzon, O., & Camilleri, K. P.. (2018). To train or not to train? a survey on training of feature extraction methods for SSVEP-based bcis. Journal of Neural Engineering, 15(5), 051001.1-051001.24.

[19] P Yuan, X Chen, Y Wang, X Gao, & S Gao. (2015). Enhancing performances of SSVEP-based brain-computer interfaces via exploiting inter-subject information.

[20] D.J. McFarland & J.R. Wolpaw. (2017).EEG-based brain–computer interfaces. Current Opinion in Biomedical Engineering. doi: 10.1016/j.cobme.2017.11.004.

[21] Wang, Z., Hu, H., Chen, X., Zhou, T., & Xu, T.. (2020). A Novel SSVEP-Based Brain-Computer Interface Using Joint Frequency and Space Modulation. IEEE INFOCOM 2020 - IEEE Conference on Computer Communications Workshops (INFOCOM WKSHPS). IEEE.

[22] Kleiner, M. B., Brainard, D. H., Pelli, D. G., Ingling, A., & Broussard, C.. (2007). What's new in psychtoolbox-3?. Perception, 36(2), 301-7.

[23] Bin, G., Lin, Z., Gao, X., Bo, H., & Gao, S.. (2008). The SSVEP topographic scalp maps by canonical correlation analysis. Conference proceedings: Annual International Conference of the IEEE Engineering in Medicine and Biology Society. IEEE Engineering in Medicine and Biology Society. Conference, 2008, 3759-3762.

[24] Zou Yuan, Nathan Viswam & Jafari Roozbeh. (2016). Automatic Identification of Artifact-Related Independent Components for Artifact Removal in EEG Recordings. IEEE journal of biomedical and health informatics (1). doi:10.1109/JBHI.2014.2370646.

[25] M Koáodziej, Majkowski, A., & Rak, R. J. . (2015). A new method of spatial filters design for brain-computer interface based on steady state visually evoked potentials. IEEE International Conference on Intelligent Data Acquisition & Advanced Computing Systems: Technology & Applications. IEEE.

[26] Zhang, W., Tan, C., Sun, F., Wu, H., & Zhang, B.. (2018). A review of EEG-based brain-computer interface systems design. Brain Science Advances, 4(2), 156-167.

[27] Moses, D. A., Leonard, M. K., Makin, J. G., and Chang, E. F. (2019). Real- time decoding of question-and-answer speech dialogue using human cortical activity. Nat. Commun. 10:3096. doi: 10.1038/s41467-019-10994-4

[28] Khan, M., Das, R., Iversen, H., and Puthusserypady, S. (2020). Review on motor imagery based BCI systems for upper limb post-stroke neurorehabilitation: from designing to application. Comput. Biol. Med. 123:103843. doi: 10.1016/j.compbiomed.2020.103843

[29] Cawley, G. C.. (2006). Leave-One-Out Cross-Validation Based Model Selection Criteria for Weighted LS-SVMs. The 2006 IEEE International Joint Conference on Neural Network Proceedings. IEEE.

Author Biographies

LI Jiaxin is a currently a M.Sc. candidate. His main research interests include deep learning and brain computer interface.

E-mail: 790861600@qq.com

DAI Fengzhi received a Ph.D. degree in engineering from Oita University in Japan in 2004. He is currently an associate professor at Tianjin University of Science and Technology. His main research interest includes artificial intelligence.

E-mail: daifz@tust.edu.cn

YIN Di main research interests include brain computer interface, pattern recognition, etc.

E-mail: yindidi1993@163.com

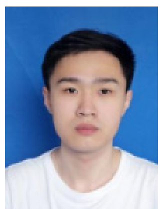

LU Peng is currently a M.Sc. candidate at Tianjin University of Science and Technology. His main research interests include multi-sensor fusion, artificial intelligence, and robotics technology.

E-mail: lupeng970504@163.com

WEN Haokang is currently a M.Sc. candidate at Tianjin University of Science and Technology. His main research interest includes digital image processing.

E-mail: 504912967@qq.com